Atmos. Chem. Phys. Discuss., 13, 11395–11425, 2013
www.atmos-chem-phys-discuss.net/13/11395/2013/
doi:10.5194/acpd-13-11395-2013

Atmospheric Chemistry and Physics Discussions

Stratospheric SO_2 and sulphate aerosol, model simulations and satellite observations

C. Brühl[1], J. Lelieveld[1,3], M. Höpfner[2], and H. Tost[4]

[1]Atmospheric Chemistry Department, Max-Planck-Institute for Chemistry, Mainz, Germany
[2]Institute for Meteorology and Climate Research, Karlruhe Institute of Technology, Karlsruhe, Germany
[3]The Cyprus Institute, Nicosia, Cyprus
[4]Institute for Physics of the Atmosphere, Johannes Gutenberg University, Mainz, Germany

Received: 28 March 2013 – Accepted: 16 April 2013 – Published: 29 April 2013

Correspondence to: C. Brühl (christoph.bruehl@mpic.de)

Published by Copernicus Publications on behalf of the European Geosciences Union.

Abstract

A multiyear study with the atmospheric chemistry general circulation model EMAC with the aerosol module GMXe at high altitude resolution demonstrates that the sulfur gases COS and SO_2, the latter from low-latitude volcanic eruptions, predominantly control the formation of stratospheric aerosol. The model consistently uses the same parameters in the troposphere and stratosphere for 7 aerosol modes applied. Lower boundary conditions for COS and other long-lived trace gases are taken from measurement networks, while estimates of volcanic SO_2 emissions are based on satellite observations. We show comparisons with satellite data for aerosol extinction (e.g. SAGE) and SO_2 in the middle atmosphere (MIPAS on ENVISAT). This corroborates the interannual variability induced by the Quasi-Biennial Oscillation, which is internally generated by the model. The model also realistically simulates the radiative effects of stratospheric and tropospheric aerosol including the effects on the model dynamics. The medium strength volcanic eruptions of 2005 and 2006 exerted a nonnegligible radiative forcing of up to $-0.6\,W\,m^{-2}$ in the tropics, while the large Pinatubo eruption caused a maximum though short term tropical forcing of about $-10\,W\,m^{-2}$. The study also shows that observed upper stratospheric SO_2 can be simulated accurately only when a sulphur sink on meteoritic dust is included and the photolysis of gaseous H_2SO_4 in the near infrared is higher than assumed previously.

1 Introduction

The relatively long atmospheric lifetime of carbonyl sulphide (COS) of > 2 yr, combined with biogenic and anthropogenic (≈ 30 %) sources, cause COS to be the most abundant atmospheric sulphur species (Montzka et al., 2007). Its lifetime is long enough so that some fraction, about $0.15\,Mt\,S\,yr^{-1}$, penetrates the stratosphere (Brühl et al., 2012). The latter study also showed that COS and its oxidation into sulphate constitute the main source of the stratospheric background aerosol (Junge layer). Hofmann et al.

ACPD
13, 11395–11425, 2013

(2009) posed that the observed increasing trend since about 2000 in stratospheric aerosol is due to anthropogenic sulphur dioxide (SO_2) from China, however, Vernier et al. (2011), Neely et al. (2013), and also this study demonstrate that SO_2 injections from medium strength tropical volcano eruptions and transport by the Brewer Dobson circulation can explain the observed increase in recent years. The almost 10 yr of SO_2 observations by the MIPAS instrument (Michelson Interferometer for Passive Atmospheric Sounding) on the ENVISAT satellite support this, indicated by the near-absence of localized maxima in the lower stratosphere of the northern subtropics apart from volcanic eruptions (Höpfner et al., 2013). This article presents calculations with a coupled lower-middle atmospheric chemistry general circulation model and a comparison of the results with satellite data to study the stratospheric sulphur cycle and its relation to radiative and dynamical processes. The impacts are most clearly illustrated by volcanic eruptions that cause transport of SO_2 into the stratosphere, in particular that by Mt. Pinatubo in 1991, which caused the largest vent of SO_2 across the tropical tropopause in the 20th century (McCormick et al., 1995).

2 Model setup

The ECHAM5 general circulation model (Roeckner et al., 2006), coupled to the Modular Earth Submodel System (MESSy, Jöckel et al., 2006) Atmospheric Chemistry (EMAC) model together with the aerosol module GMXe (Pringle et al., 2010) with 7 aerosol modes was applied in this study. The spectral model resolution applied is T42, i.e. about 2.8° in latitude and longitude. The vertical grid structure resolves the lower and middle atmosphere with 90 layers from the surface to a top layer centred at 0.01 hPa (Giorgetta et al., 2006). In this setup an internally consistent Quasi-Biennial Oscillation (QBO) is generated, being close to the observations for the 9 yr analysed. Lower boundary conditions for the different aerosol types are as described in Pringle et al. (2010). Volcanic SO_2 is injected by adding the observed SO_2 masses in a zonally averaged plume derived from satellite data within a few weeks after the actual eruption.

ACPD
13, 11395–11425, 2013

As in Brühl et al. (2012) sedimentation of aerosol particles is calculated with a Walcek scheme described by Benduhn and Lawrence (2013). Aerosol extinction is calculated from Mie theory using pre-calculated look-up tables for the 6 aerosol components water, water soluble species (including sulphuric acid and sulphate aerosol), organic carbon, black carbon, mineral dust and sea salt. The radiation module can be used to perform additional diagnostic calculations of radiative forcing and heating rate anomalies for different aerosol options. Simulations have been performed with and without coupling of the aerosol heating to the model dynamics. To distinguish aerosol chemical and dynamical effects radiative feedbacks of ozone changes have been switched off here. Different from Brühl et al. (2012), where further details can be found, in most simulations shown here the boundary between acccumulation mode and coarse mode was shifted (to 1.6 µm) to remedy the overestimation of sedimentation by large particles for the Pinatubo case. Nevertheless, the tropospheric burdens of the different aerosol types and the total aerosol optical depth are close to those calculated by Pringle et al. (2010), which indicates that this size definition is important mostly for the relatively low air density in the stratosphere.

3 Stratospheric aerosol and its radiative impact, including volcanoes

3.1 The Pinatubo eruption

The eruption of Pinatubo in June 1991 was the strongest in the last century, which has been well documented, and is used here as a test case for the model. The volcano injected about 20 Mt SO_2 (Table 1) into the stratosphere up to about 30 km altitude (McCormick et al., 1995). The formation of sulphate aerosol peaked around 27 km as observed by SAGE (Thomason et al., 1997). In the model simulation the whole amount of SO_2 was injected at 1 September with the altitude and latitude distribution of the aerosol according to SAGE (Stratospheric Aerosol and Gas Experiment) data. Because the SAGE data contain gaps due to detector saturation, two estimates for the

ACPD
13, 11395–11425, 2013

initial Pinatubo SO_2 distribution in the simulations were used. The high estimate with about 20.6 Mt applies the maximum values at each gridpoint in the period from June to September 1991, the low estimate with about 14 Mt takes the September values with some extrapolation into the region without data using an older data version. In the following we focus on results with the high estimate which is closer to the estimates of total injected SO_2 in the literature and closer to the observed time evolution of volcanic aerosol. Figure 1 shows the temporal development of SO_2, including the lofting by the Brewer Dobson circulation with and without radiative feedback on dynamics. The vertical profile for the simulation with dynamical coupling (enhanced photolysis of gaseous H_2SO_4 and a sink on meteoric dust are included, discussed below), is close to the ATMOS observations in April 1992 (about 0.5 ppbv above 40 km) and April 1993 (Rinsland et al., 1995) and the MLS/UARS observations (Read et al, 1993).

After about 1 month most of the SO_2 in the middle and lower stratosphere is converted to sulphate aerosol, mostly residing in the accumulation mode. The aerosol removal by sedimentation takes about 2 yr, somewhat faster than observed as can be seen in Fig. 2, which shows the corresponding extinction in the simulation results and observations in the tropics. Inclusion of the effects of the volcanic radiative heating on the model dynamics in this simulation causes an enhancement of the Brewer Dobson circulation, which leads to a further lofting of the aerosol and a longer residence time, in better agreement with the observations. As can be seen from the lower panel of Fig. 2, ignoring the radiative coupling to dynamics reduces the extinction in the upper part of the aerosol layer considerably.

Figure 3 shows the aerosol radiative heating and the resulting changes in temperature and stratospheric water vapour in the simulations with coupling. The temperature changes of up to 7 K at 24 km are consistent with observations (McCormick et al., 1995). Since we compare two (three including the low estimate) free running simulations of a GCM, the significance of the volcanic signal decreases with time relative to the meteorological variability (noise). Our results show stronger radiative heating at about 27 km than Stenchikov et al. (1998) while our calculated heating near the

ACPD
13, 11395–11425, 2013

tropopause is less, which is consistent with recent findings of Arfeuille et al. (2013). The largest heating by volcanic aerosol in the tropical tropopause region occurs about 9 months after the injection as a consequence of particle sedimentation. This leads to a less efficient cold trap for water vapour and an increase of about 0.5 ppmv, propagating upward with the "tape recorder" (Fig. 3), again consistent with observations ((e.g. SPARC, 2000)). The cooling at the top of the aerosol layer after some months is related to a slight shift in the phase of the QBO compared to the simulation without radiative feedback (Fig. 4). The local changes in zonal wind due to this shift can be rather large.

The sulphate aerosol volume mixing ratio is shown in Fig. 5. The conversion of SAGE surface area densities to sulphate volume mixing ratios has been done with the empirical formula by Grainger et al. (1995), but different from Brühl et al. (2012), including an altitude dependent correction for humidity (based on Carslaw et al., 1995). The corresponding total sulphate burdens in Fig. 6 are given for both estimates. Note that in the first 6 months after the eruption SAGE data are low biased because the data gaps due to saturation are not filled with extrapolations here. In the simulations a fraction of up to about 1 ppbv in the coarse mode causes a somewhat too fast removal of aerosol by sedimentation. However, shifting the mode boundary to larger radii to reduce this fraction makes the model results deviate too strongly from observations in the troposphere (we aim for a consistent model representation of aerosols in the lower and the middle atmosphere). In the model Pinatubo cloud particles in the accumulation mode have a typical wet radius of 0.3 µm. In the coarse mode the radius can grow to 2 to 5 µm in the lowermost tropical stratosphere.

The simulated solar and total radiative forcing of the Pinatubo aerosol at the tropopause is shown in Fig. 7. The maximum negative forcing in excess of $10\,W\,m^{-2}$ for the high estimate is somewhat larger than the satellite derived value of $8\,W\,m^{-2}$ reported by McCormick et al. (1995). However, this is based on an outdated data version (Arfeuille et al., 2013). Globally averaged the calculated forcing peaks at $6.5\,W\,m^{-2}$ in December 1991, decreasing to $1.3\,W\,m^{-2}$ in December 1992 and $0.25\,W\,m^{-2}$ in December 1993 (not shown). This decrease appears to be faster than that reported by

ACPD
13, 11395–11425, 2013

Solomon et al. (2011) indicating that the forcing should be back to 0.25 $W m^{-2}$ one year after that simulated by our model.

3.2 Background and medium size tropical volcano eruptions

The simulation of Brühl et al. (2012), from which COS was identified as the main source for stratospheric background aerosol, was continued for an additional 5 yr, including the SO_2 release from 4 medium strength volcanic eruptions into the tropical stratosphere. The SO_2 of Nyiragongo, Manam and Soufriere Hills was injected at around 20 km while the injection by Rabaul occured around 18 km, inferred from the TOMS derived masses given in Table 1 and satellite data shown in Vernier et al. (2011). These assumptions agree with MIPAS observations (see Sect. 4). The corresponding aerosol volume mixing ratios are depicted in Fig. 8, using again the improved conversion formula for the SAGE data. At around 29 km altitude the simulated aerosol is still low by 20 to 30 % but below about 25 km with the more appropriate conversion formula the model is now very close to the observations. The simulated QBO, which nearly follows the observations in the shown period, modulates the sulphate distribution. As in Brühl et al. (2012) by accounting for the calculated particulate organic carbon, transported from the troposphere, the agreement with observations in the lower stratosphere (Thomason et al., 2008) is much improved. Figure 9 shows the time-series of total stratospheric burdens indicating that the model agrees well with the SAGE derived values at times of full coverage (maxima in the figure). Here also the use of the adjusted conversion formula leeds to a significant improvement compared to Brühl et al. (2012). The calculated typical wet particle radius in the accumulation mode is about 0.1 µm, in the volcanic plumes it can increase to about 0.17 µm.

Simulated and observed extinction are shown in Fig. 10. In the middle stratosphere the simulated extinction is somewhat lower than in the SAGE data, consistent with Fig. 8. The difference might be due to the fact that the model does not include effects of meteoritic smoke (Neely et al., 2011) in the extinction and radiation calculations, which

ACPD
13, 11395–11425, 2013

are included in the satellite data, though not distinct from sulphate. Figure 11 shows the total radiative heating due to the volcanic aerosol without coupling to dynamics and the radiative forcing by aerosol in the model. The forcing of −0.2 to −0.6 $W m^{-2}$ in low latitudes and −0.1 to −0.3 $W m^{-2}$ globally averaged by the medium size volcanoes might have contributed to the observed stagnation in global temperature increase in the past decade (Solomon et al., 2011). Aerosol heating rates and corresponding temperature changes in a sensitivity study including the feedback of the aerosol onto the meteorology are presented in Fig. 12. The signal of the first volcano is clearly visible while for the second one temperature changes due to changes in dynamics of the two free running simulations are of the same order of magnitude as the volcanic signal. Even for the first volcano it appears that in the model the vertical winds respond first to radiative heating, masking a direct temperature increase by adiabatic cooling.

4 Stratospheric SO_2, simulations and MIPAS observations

Sporadic measurements by the ATMOS instrument on the Space Shuttle (Rinsland et al., 1995) show that SO_2 increases with altitude in the upper stratosphere and that it is enhanced after major volcanic eruptions like Pinatubo in 1991 (see Fig. 1). After a long period without spaceborne measurements the MIPAS instrument on ENVISAT provided data from 2002 to 2012 (Höpfner et al., 2013). Figure 13 shows a comparison of the EMAC simulations with these data. In the observations the volcano induced SO_2 peaks around 18 to 20 km are low-biased because of averaging over a longer period and because no satellite retrieval is possible when strongly enhanced sulphate aerosol or volcanic ash is present. Individual MIPAS data points and also zonal averages based on them are well above 1 ppbv around the plumes of Manam, Soufriere Hills and Rabaul (see Table 1). The calculated and observed SO_2 distribution with latitude at 22 km is given in Fig. 14. The peaks in the tropics show that the volcanic material is transported upward with the Brewer Dobson circulation. In the simulation the transport to midlatitudes appears to be somewhat too fast. The delay of the peak

ACPD
13, 11395–11425, 2013

around December 2002 is a consequence of injecting the SO_2 of 3 subsequent eruptions together in the model at the 1 January 2003. From analysis of the individual MIPAS data it can be inferred that the continuously enhanced tropical values are mostly due to smaller volcanic eruptions not taken into account in the model. However, as shown by Tost et al. (2010) the model tends to underestimate upper tropospheric SO_2 and consequently sulphur injection into the lower stratosphere, as wet removal processes are too efficient. This is mostly caused by neglecting the rentention processes during droplet freezing. In the lower stratosphere over the Pacific Ocean up to a few pptv of SO_2 (locally even 10 pptv) may be related to the oxidation of marine dimethyl sulphide (DMS) transported across the tropical tropopause region by deep convection, as indicated by a sensitivity study with EMAC (not shown).

The secondary maximum at about 29 km, at the top of the Junge layer, is present in both, observations and simulations. In the upper stratosphere relatively high values, as also shown by the observations (Fig. 13), are simulated with the setup of Brühl et al. (2012) and appear some kilometers higher. Mills et al. (2005) also simulate relatively low SO_2 at about 40 km and too high SO_2 at altitudes above about 50 km compared to observations. They discuss the need to account for a sink of total sulphur by reactions on meteoritic smoke particles and also the sensitivity of the SO_2 to H_2SO_4 ratio on the H_2SO_4 photolysis rate in the visible and the near infrared. In the setup of Brühl et al. (2012) only the absorption bands at 742 and 608 nm of Vaida et al. (2003) were considered. Additionally assuming that the band at 966 nm leads to the photolysis of H_2SO_4 with a yield of about 20 % brings SO_2 at 40 km close to the observations in the tropics. The UV-photolysis of the intermediate SO_3 introduces also some dependence on the 11 yr solar cycle as tentatively seen by MIPAS (Fig. 13, middle panel and Höpfner et al., 2013). However, to obtain a realistic decrease of SO_2 with altitude above about 45 km and a realistic distribution with latitude also at lower altitudes, the meteoritic dust sink is needed as demonstrated by a sensitivity study with a uniform first order sink of $2.4 \times 10^{-8}\,s^{-1}$ for gaseous H_2SO_4 (Figs. 15, 16). In the sensitivity study the meteoritic particle sink, based on the tropical dust surface area densities of Bardeen et al.

ACPD
13, 11395–11425, 2013

(2008) and an assumed sticking coefficient of 0.01, is introduced at 1 July 2002, after which the sulphur species in the model adjust during about one year. The latitudinal and seasonal dependence provided by Bardeen et al. (2008) is secondary for the heterogeneous removal of gaseous H_2SO_4 because most of this species resides in the tropical middle stratosphere (Brühl et al., 2012). The much improved SO_2 results in the simulations including enhanced photolysis and a sulphur sink on meteoric dust in Figs. 13–16 demonstrate how important new satellite observations can be for model development.

5 Conclusions

The transport of COS from the troposphere and volcanic eruptions in the tropics explain most of the observed stratospheric aerosol load as well as SO_2 concentrations. Penetration of significant amounts of anthropogenic SO_2 into the stratosphere appears unlikely, apparent from the MIPAS data and the model simulations, and is not needed to explain observed aerosol distributions and trends. The comparison of model calculations that include and neglect coupling of aerosol radiative effects to dynamics shows that radiative heating anomalies, e.g. by the strong Mt. Pinatubo eruption, significantly influence the Brewer–Dobson circulation and the stratospheric aerosol lifetime. The associated aerosol radiative heating increased water vapour transport across the tropical tropopause and influenced the zonal wind, including a slight shift of the QBO. By accounting for the small source of organic aerosol through transport from the troposphere, we obtain much improved modelled aerosol extinction compared to satellite data. To realistically simulate the distribution of sulphur species in the upper stratosphere the photolysis of H_2SO_4 in the visible and near infrared is critical. Laboratory studies on the quantum yields, especially of near infrared absorption, would be useful. The impact of meteoritic smoke and dust is still mostly based on about 30 yr old studies (Hunten et al., 1980; Turco et al., 1981) with large uncertainties. The analysis of recent satellite data would be important to provide improved estimates on its source,

ACPD
13, 11395–11425, 2013

the particle size and the altitude distribution. The studies by Hervig et al. (2009) and Neely et al. (2011) are a good starting point. Inclusion of the oxidation of marine DMS causes a slight increase of sulphate aerosol in the lowermost tropical stratosphere. For the stratospheric aerosol layer the latter source is not significant and can be neglected as in most of our simulations, in contrast to the conclusion of Marandino et al. (2012). Our model simulations corroborate the importance of recent medium strength tropical volcanoes for the sulphur loading of the stratosphere. The radiative forcing of the sulphate aerosols caused by these volcanoes may have contributed to the observed slowdown of the global warming in the past decade.

Acknowledgements. The computations have been performed at the blizzard supercomputer at DKRZ, Hamburg, Germany. The sulphur injections from the volcanoes were estimated from the NASA SO_2-database at GSFC (http://so2.gsfc.nasa.gov). The research leading to these results has received funding from the European Research Council under the European Union's Seventh Framework Programme (FP7/2007-2013)/ERC grant agreement nr. 226144.

The service charges for this open access publication
have been covered by the Max Planck Society.

References

Arfeuille, F., Luo, B. P., Heckendorn, P., Weisenstein, D., Sheng, J. X., Rozanov, E., Schraner, M., Brönnimann, S., Thomason, L. W., and Peter, T.: Uncertainties in modelling the stratospheric warming following Mt. Pinatubo eruption, Atmos. Chem. Phys. Discuss., 13, 4601–4635, doi:10.5194/acpd-13-4601-2013, 2013. 11400

Bardeen, C. G., Toon, O. B., Jensen, E. J., Marsh, D. R., and Harvey, V. L.: Numerical simulations of the three-dimensional distribution of meteoric dust in the mesosphere and upper stratosphere, J. Geophys. Res., 113, D17202, doi:10.1029/2007JD009515, 2008. 11403, 11404

Benduhn, F. and Lawrence, M. G.: An investigation of the role of sedimentation for stratospheric climate engineering, J. Geophys. Res., in review, 2013. 11398

ACPD
13, 11395–11425, 2013

Brühl, C., Lelieveld, J., Crutzen, P. J., and Tost, H.: The role of carbonyl sulphide as a source of stratospheric sulphate aerosol and its impact on climate, Atmos. Chem. Phys., 12, 1239–1253, doi:10.5194/acp-12-1239-2012, 2012. 11396, 11398, 11400, 11401, 11403, 11404, 11424

Carslaw, K. S., Luo, B., and Peter, T.: An analytical expression for the composition of aqueous HNO_3-H_2SO_4 stratospheric aerosols including gas phase removal of HNO_3, Geophys. Res. Lett., 22, 1877–1880, 1995. 11400

Grainger, R. G., Lambert, A., Rodgers, C. D., Taylor, F. W., and Deshler, T.: Stratospheric aerosol effective radius, surface area and volume estimated from infrared measurements, J. Geophys. Res., 100, 16507–16518, 1995. 11400, 11414, 11417

Giorgetta, M. A., Manzini, E., Roeckner, E., Esch, M., and Bengtsson, L.: Climatology and forcing of the quasi-biennial oscillation in the MAECHAM5 model, J. Climate, 19, 3882–3901, 2006. 11397

Hervig, M. E., Gordley, L. L., Deaver, L. E., Siskind, D. E., Stevens, M. H., Russell III, J. M., Bailey, S. M., Megner, L., and Bardeen, C. G.: First satellite observations of meteoric smoke in the middle atmosphere, Geophys. Res. Lett., 36, L18805, doi:10.1029/2009GL039737, 2009. 11405

Höpfner, M., Glatthor, N., Grabowski, U., Kellmann, S., Kiefer, M., Linden, A., Orphal, J., Stiller, G., von Clarmann, T., and B. Funke: Sulphur dioxide (SO_2) as observed by MIPAS/Envisat: temporal development and spatial distribution at 15–45 km altitude, Atmos. Phys. Chem. Discuss., in review, 2013. 11397, 11402, 11403

Hofmann, D., Barnes, J., O'Neill, M., Trudeau, M., and Neely, R.: Increase in background stratospheric aerosol observed with lidar at Mauna Loa Observatory and Boulder, Colorado, Geophys. Res. Lett., 36, L15808, doi:10.1029/2009GL039008, 2009. 11396

Hunten, D. M., Turco, R. P., and Toon, O. B.: Smoke and dust particles of meteoric origin in the mesosphere and stratosphere, J. Atmos. Sci., 37, 1342–1357, 1980. 11404

Jöckel, P., Tost, H., Pozzer, A., Brühl, C., Buchholz, J., Ganzeveld, L., Hoor, P., Kerkweg, A., Lawrence, M. G., Sander, R., Steil, B., Stiller, G., Tanarhte, M., Taraborrelli, D., van Aardenne, J., and Lelieveld, J.: The atmospheric chemistry general circulation model ECHAM5/MESSy1: consistent simulation of ozone from the surface to the mesosphere, Atmos. Chem. Phys., 6, 5067–5104, doi:10.5194/acp-6-5067-2006, 2006. 11397

Kley, D., Russell III, J. M. and Phillips, C. (Eds.): SPARC assessment of upper tropospheric and stratospheric water vapour, WCRP-113, SPARC report No. 2, 2000. 11400

ACPD
13, 11395–11425, 2013

Marandino, C. A., Tegtmeier, S., Krüger, K., Zindler, C., Atlas, E. L., Moore, F., and Bange, H. W.: Dimethylsulphide (DMS) emissions from the West Pacific Ocean: a potential marine source for the stratospheric sulphur layer, Atmos. Chem. Phys. Discuss., 12, 30543–30570, doi:10.5194/acpd-12-30543-2012, 2012. 11405

McCormick, M. P., Thomason, L. W., and Trepte, C. R.: Atmospheric effects of the Mt. Pinatubo eruption, Nature, 373, 399–404, 1995. 11397, 11398, 11399, 11400

Mills, M. J., Toon, O. B., Vaida, V., Hintze, P. E., Kjaergaard, H. G., Schofield, D. P., and Robinson, T. W.: Photolysis of sulfuric acid vapor by visible light as a source of the polar stratospheric CN layer, J. Geophys. Res., 110, D08201, doi:10.1029/2004JD005519, 2005. 11403

Montzka, S. A., Calvert, P., Hall, B. D., Elkins, J. W., Conway, T. J., Tans, P. P., and Sweeney, C.: On the global distribution, seasonality, and budget of atmospheric carbonyl sulfide and some similarities with CO_2, J. Geophys. Res., 112, D09302, doi:10.1029/2006JD007665, 2007. 11396

Neely III, R. R., English, J. M., Toon, O. B., Solomon, S., Mills, M., and Thayer, J. P.: Implications of extinction due to meteoritic smoke in the upper stratosphere, Geophys. Res. Lett., 38, L24808, doi:10.1029/2011GL049865, 2011. 11401, 11405

Neely III, R. R., Toon, O. B., Solomon, S., Vernier, J. P., Alvarez, C., English, J. M., Rosenlof, K. H., Mills, M., Bardeen, C. G., Daniel, J. S., and Thayer, J. P.: Recent anthropogenic increases in SO_2 from Asia have minimal impact on stratospheric aerosol, Geophys. Res. Lett., 40, doi:10.1002/grl.50263, in press, 2013. 11397

Pringle, K. J., Tost, H., Message, S., Steil, B., Giannadaki, D., Nenes, A., Fountoukis, C., Stier, P., Vignati, E., and Lelieveld, J.: Description and evaluation of GMXe: a new aerosol submodel for global simulations (v1), Geosci. Model Dev., 3, 391–412, doi:10.5194/gmd-3-391-2010, 2010. 11397, 11398

Pringle, K. J., Tost, H., Metzger, S., Steil, B., Giannadaki, D., Nenes, A., Fountoukis, C., Stier, P., Vignati, E., and Lelieveld, J.: Corrigendum to "Description and evaluation of GMXe: a new aerosol submodel for global simulations (v1)" published in Geosci. Model Dev., 3, 391–412, 2010, Geosci. Model Dev., 3, 413–413, doi:10.5194/gmd-3-413-2010, 2010.

Read, W. G., Froidevaux, L., and Waters, J. W.: Microwave Limb Sounder measurements of stratospheric SO_2 from the Mt. Pinatubo volcano, Geophys. Res. Lett., 20, 1299–1302, 1993. 11399

ACPD
13, 11395–11425, 2013

Rinsland, C. P., Gunson, M. R., Ko, M. K. W., Weisenstein, D. W., Zander, R., Abrams, M. C., Goldman, A., Sze, N. D., and Yue, G. K.: H_2SO_4 photolysis: a source of sulfur dioxide in the upper stratosphere, Geophys. Res. Lett., 22, 1109–1112, 1995. 11399, 11402

Roeckner, E., Brokopf, R., Esch, M., Giorgetta, M., Hagemann, S., Kornblueh, L., Manzini, E., Schlese, U., and Schulzweida, U.: Sensitivity of simulated climate to horizontal and vertical resolution in the ECHAM5 atmosphere model, J. Climate, 19, 3771–3791, 2006. 11397

Solomon, S., Daniel, J. S., Neely III, R. R., Vernier, J.-P., Dutton, E. G., and Thomason, L. W.: The persistently variable "background" stratospheric aerosol layer and global climate change, Science, 333, 866–870, 2011. 11401, 11402

Stenchikov, G. L., Kirchner, I., Robock, A., Graf, H.-F., Antuña, J. C., Grainger, R. G., Lambert, A., and Thomason, L.: Radiative forcing from the 1991 Mount Pinatubo volcanic eruption, J. Geophys. Res., 103, 13837–13857, 1998. 11399

Thomason, L. W., Poole, L. R., and Deshler, T.: A global climatology of stratospheric aerosol surface area density deduced from Stratospheric Aerosol and Gas Experiment II measurements: 1984–1994, J. Geophys. Res., 102, 8967–8976, 1997. 11398

Thomason, L. W., Burton, S. P., Luo, B.-P., and Peter, T.: SAGE II measurements of stratospheric aerosol properties at non-volcanic levels, Atmos. Chem. Phys., 8, 983–995, doi:10.5194/acp-8-983-2008, 2008. 11401

Tost, H., Lawrence, M. G., Brühl, C., Jöckel, P., The GABRIEL Team, and The SCOUT-O3-DARWIN/ACTIVE Team: Uncertainties in atmospheric chemistry modelling due to convection parameterisations and subsequent scavenging, Atmos. Chem. Phys., 10, 1931–1951, doi:10.5194/acp-10-1931-2010, 2010. 11403

Turco, R. P., Toon, O. B., Hamill, P., and Whitten, R. C.: Effects of meteoric debris on stratospheric aerosol and gases, J. Geophys. Res., 86, 1113–1128, 1981. 11404

Vaida, V., Kjaergaard, H. G., Hintze, P. E., and Donaldson, D. J.: Photolysis of sulfuric acid vapor by visible solar radiation, Science, 299, 1566–1568, 2003. 11403

Vernier, J.-P., Thomason, L. W., Pommereau, J. P., Bourassa, A., Pelon, J., Garnier, A., Hauchecorne, A., Blanot, L., Trepte, C., Degenstein, D., and Vargas, F.: Major influence of tropical volcanic eruptions on the stratospheric aerosol layer during the last decade, Geophys. Res. Lett., 38, L12807, doi:10.1029/2011GL047563, 2011. 11397, 11401

ACPD
13, 11395–11425, 2013

Table 1. Maximum SO_2 mass (in kt) from volcanoes applied in the model, estimated from TOMS on Nimbus, Earthprobe and OMI (+ indicates inclusion of other volcanoes erupting at the same time at other longitudes).

Volcano	SO_2
Pinatubo (Jun 1991)	20 600
Nyiragongo + (Nov, Dec 2002)	48
Manam (Jan 2005)	136
Soufriere Hills (May 2006)	196
Rabaul (Oct 2006)	281

ACPD
13, 11395–11425, 2013

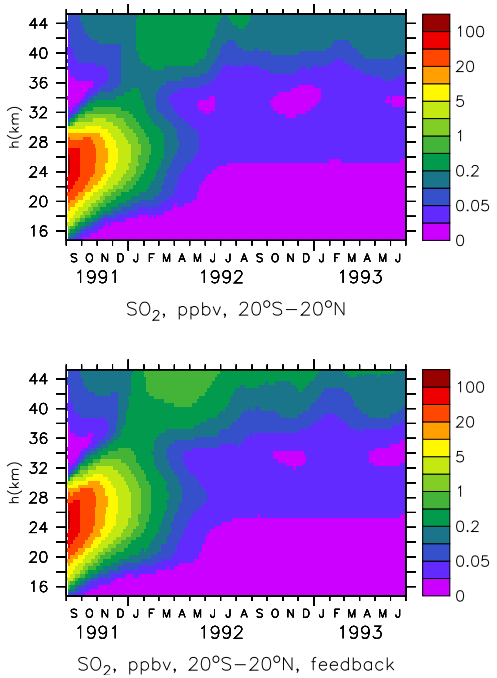

Fig. 1. Simulated SO_2 in the tropical stratosphere (volume mixing ratio) after the Pinatubo eruption, without and with coupling to dynamics. Enhanced H_2SO_4 photolysis and meteoric sink are included.

ACPD
13, 11395–11425, 2013

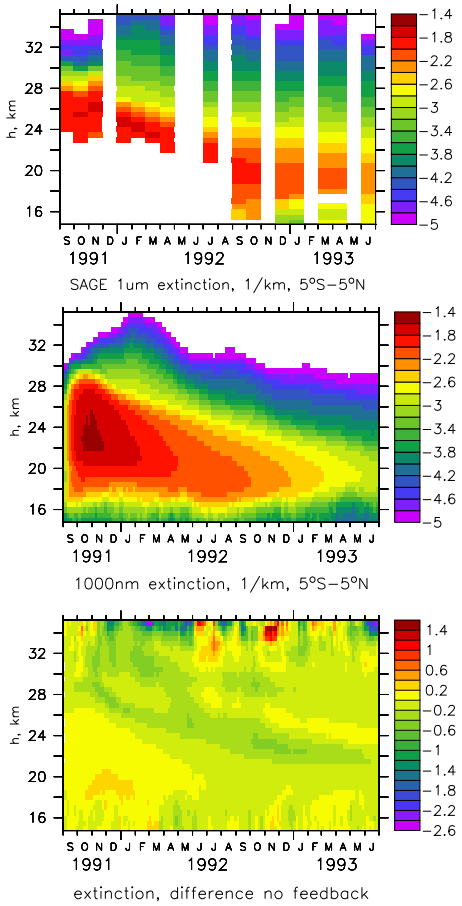

Fig. 2. SAGE observed and simulated extinction at 1 µm (decadal logarithm) after the Pinatubo eruption (with radiative coupling to dynamics). Lower panel shows the difference of the decadal logarithms of the simulation without coupling and the one with coupling.

ACPD
13, 11395–11425, 2013

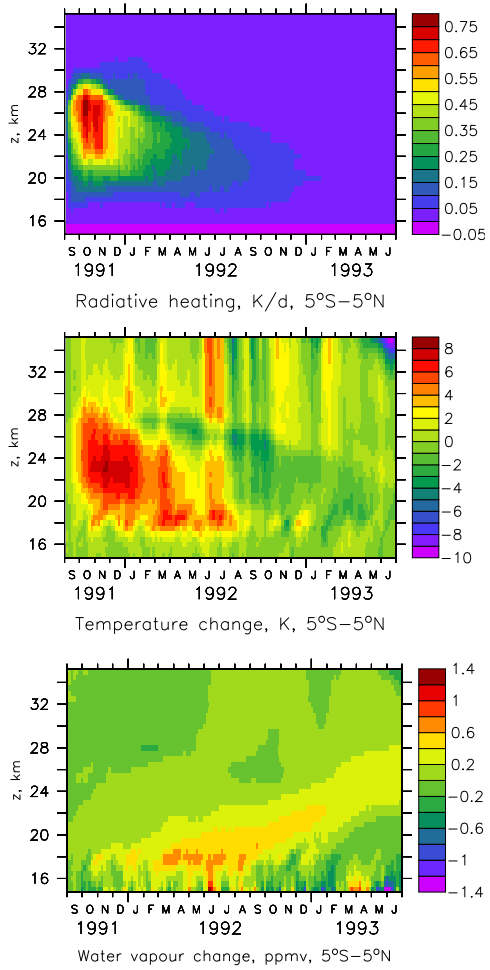

Fig. 3. Radiative heating, temperature and water vapour change due to Pinatubo aerosol.

ACPD
13, 11395–11425, 2013

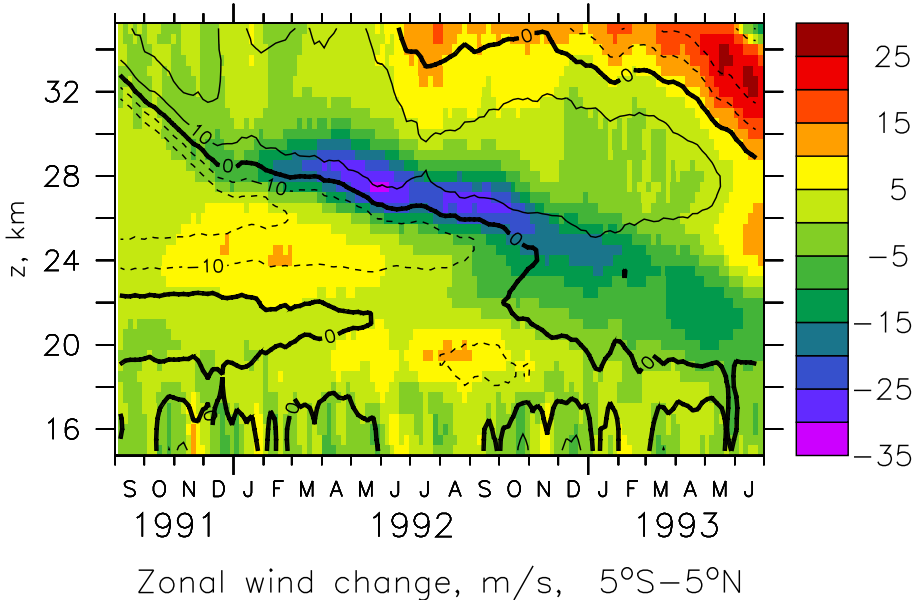

Fig. 4. Change in zonal wind (QBO) due to radiative coupling to dynamics after Pinatubo; contours zonal wind of simulation without coupling.

ACPD
13, 11395–11425, 2013

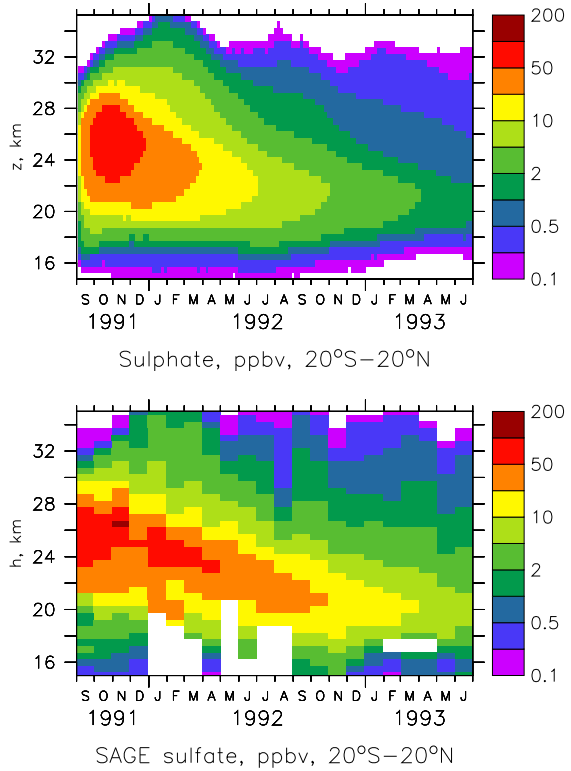

Fig. 5. Sulphate volume mixing ratios as simulated (upper panel, with coupling to dynamics) and estimated from SAGE observations (lower panel) with corrected formula by Grainger et al. (1995).

ACPD
13, 11395–11425, 2013

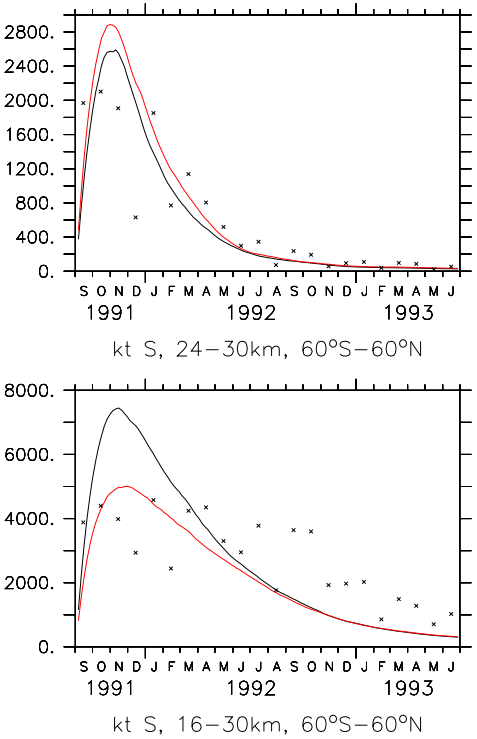

Fig. 6. Stratospheric sulphur burden; black is calculated by EMAC (high estimate), red EMAC (low estimate), symbols estimated from SAGE (low in the beginning due to data gaps).

ACPD
13, 11395–11425, 2013

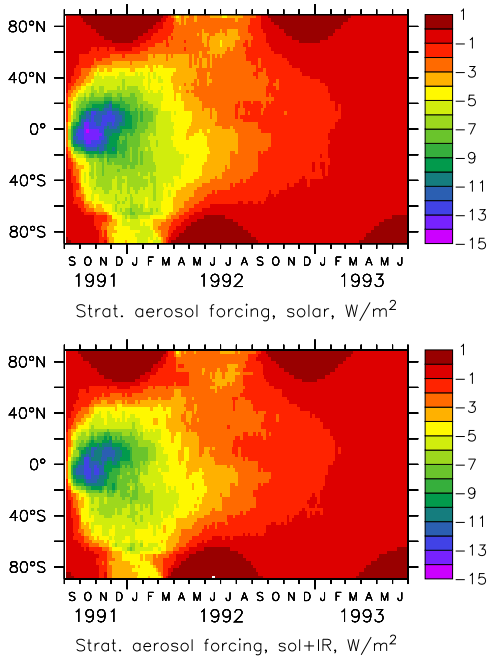

Fig. 7. Solar and total radiative forcing due to Pinatubo aerosols (at about tropopause, 185 hPa).

ACPD
13, 11395–11425, 2013

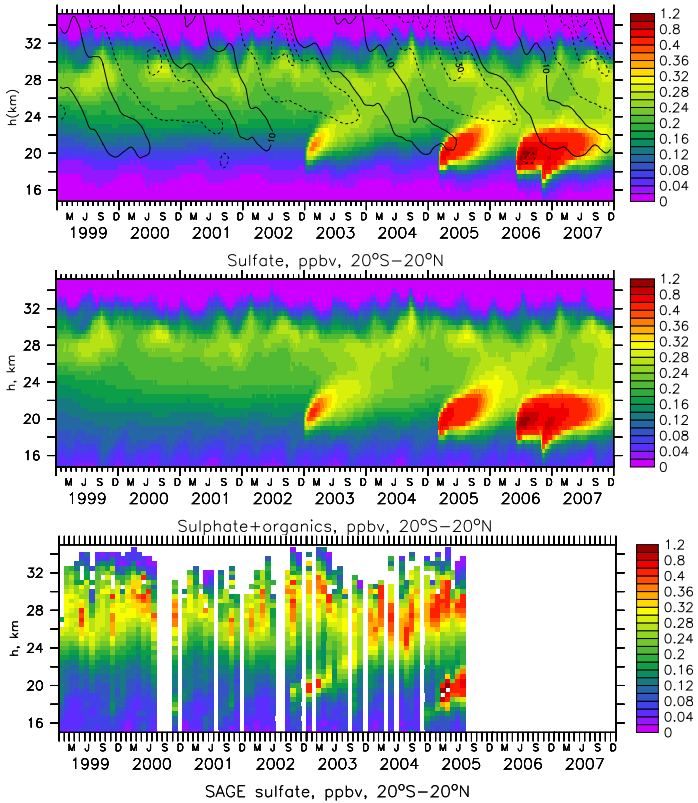

Fig. 8. Simulated and SAGE observed aerosol (as volume mixing ratio). The SAGE values (lower panel) are based on surface area density and the conversion formula by Grainger et al. (1995) with an empirical correction for water. The contours of zonal wind indicate the QBO (in steps of 20 m s^{-1}, 5° S–5° N). The upper panel shows simulated sulphate aerosol and the middle panel additionally particulate organic matter.

ACPD
13, 11395–11425, 2013

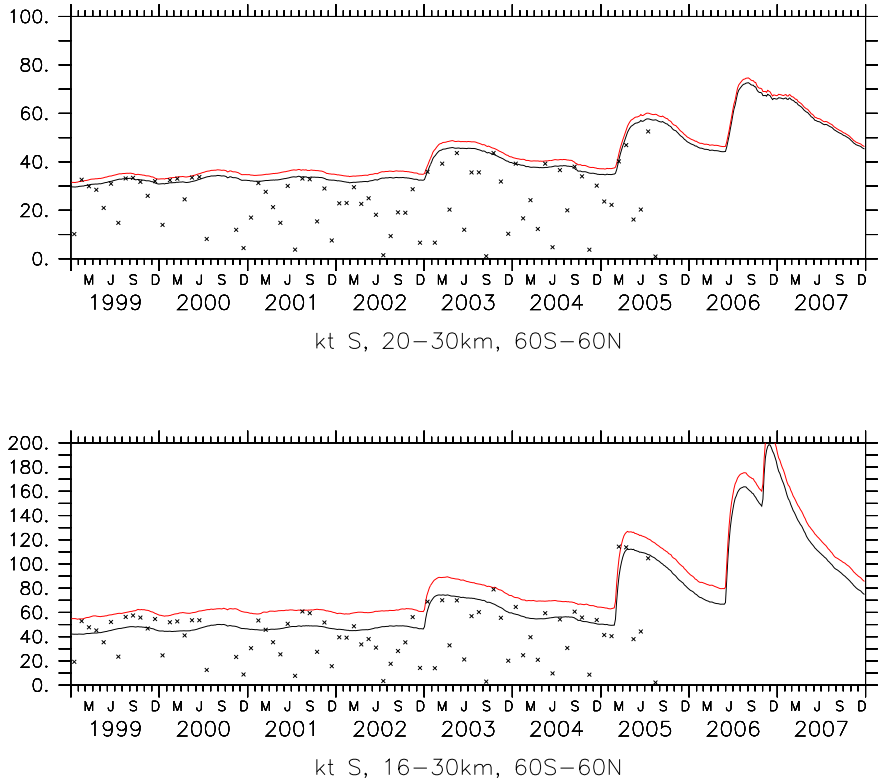

Fig. 9. Stratospheric sulphur burden, black lines calculated by EMAC, red including the (mass scaled) contribution by particulate organic carbon. Symbols derived from SAGE surface area densities (low values are due to incomplete coverage of the latitude range).

ACPD
13, 11395–11425, 2013

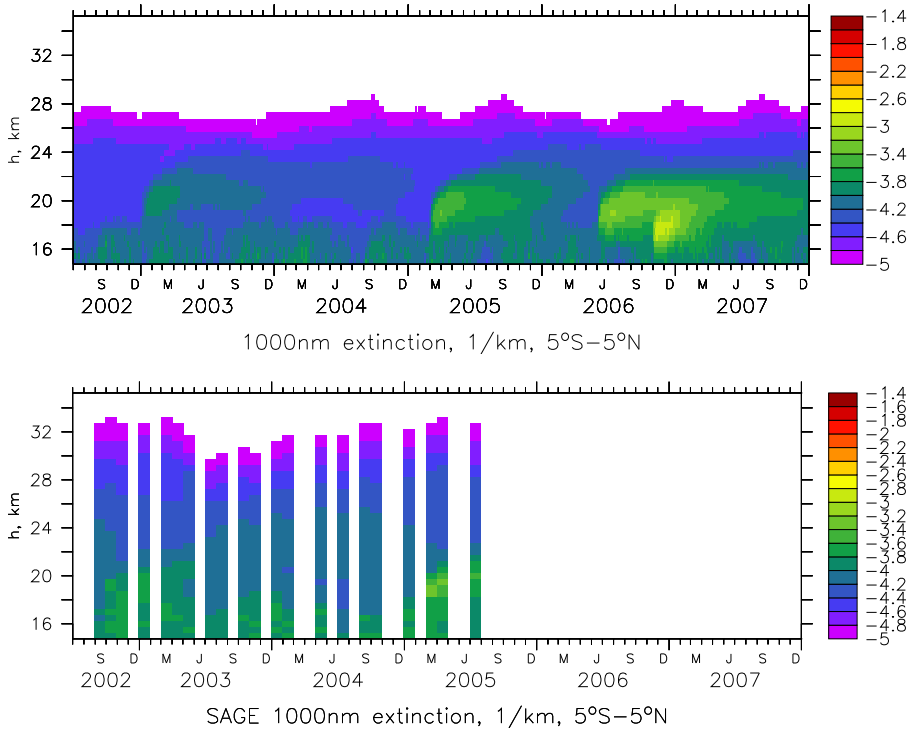

Fig. 10. Simulated and observed extinction at 1 µm, tropics.

ACPD
13, 11395–11425, 2013

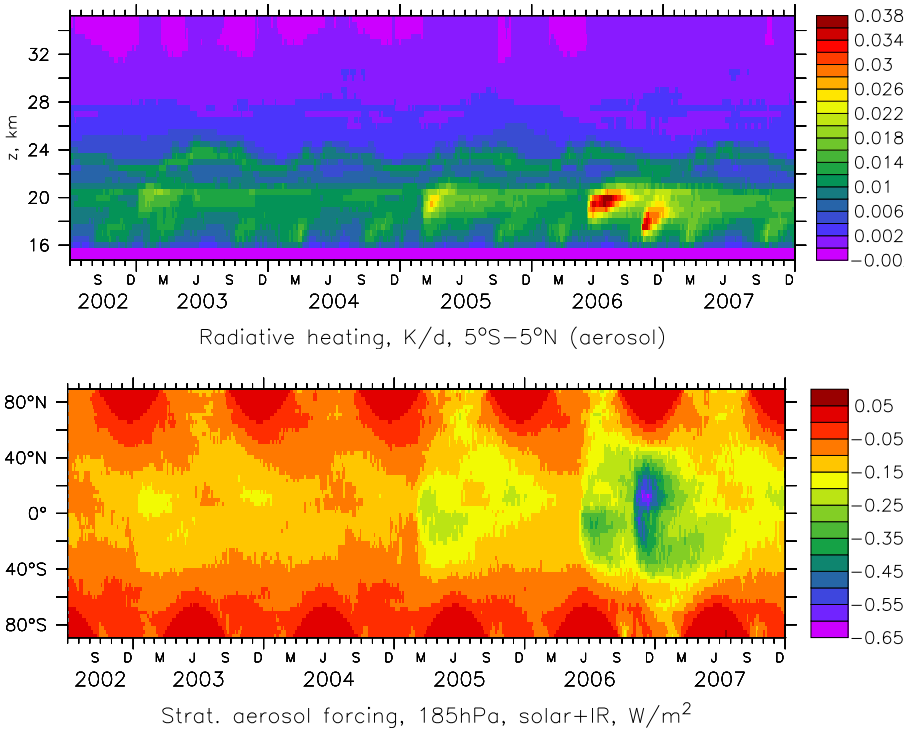

Fig. 11. Radiative heating by stratospheric aerosol in the tropics (upper panel, no feedback) and total radiative forcing across latitudes at 185 hPa (tropopause, lower panel).

ACPD
13, 11395–11425, 2013

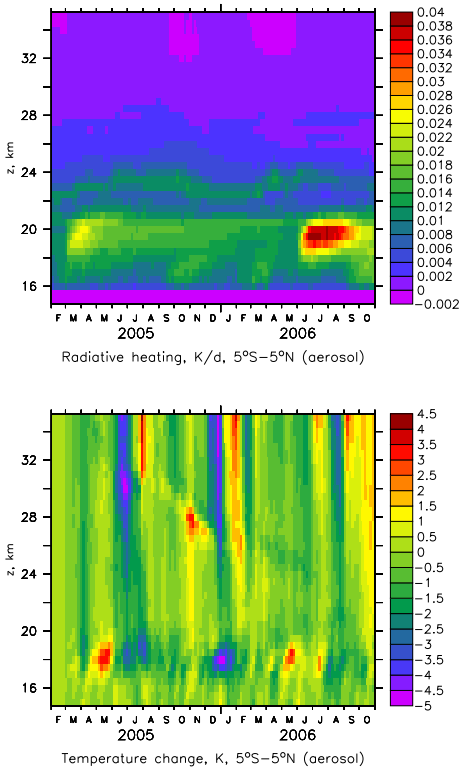

Fig. 12. Radiative heating and temperature change due to background aerosol and medium strength tropical volcano eruptions.

ACPD
13, 11395–11425, 2013

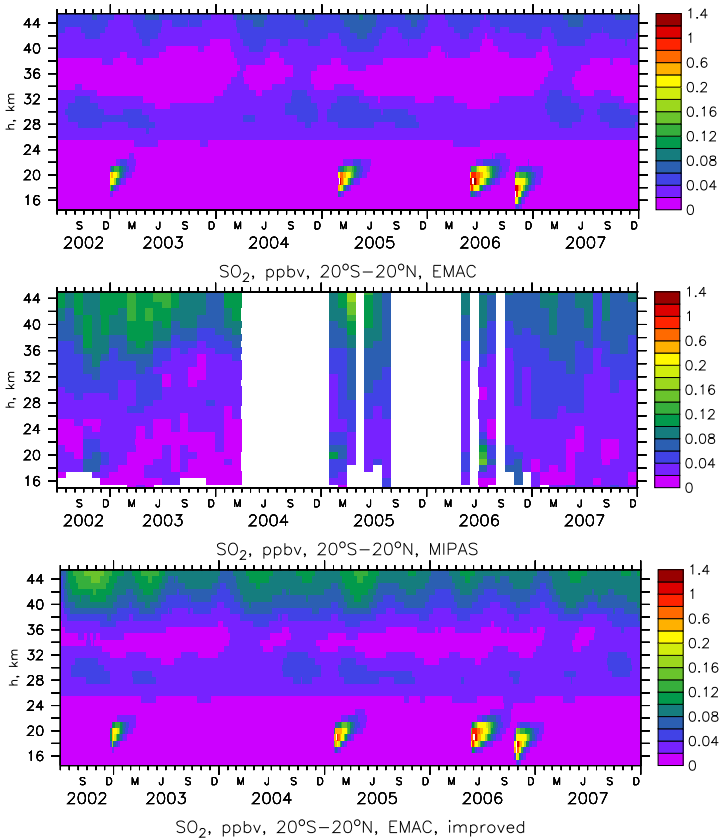

Fig. 13. Simulated and observed SO_2 in the tropical stratosphere (volume mixing ratio). Lower panel shows simulation with enhanced H_2SO_4 photolysis and sulphur sink on meteoric dust. MIPAS observations (middle panel) are monthly averaged, model data are 5 day averages.

ACPD
13, 11395–11425, 2013

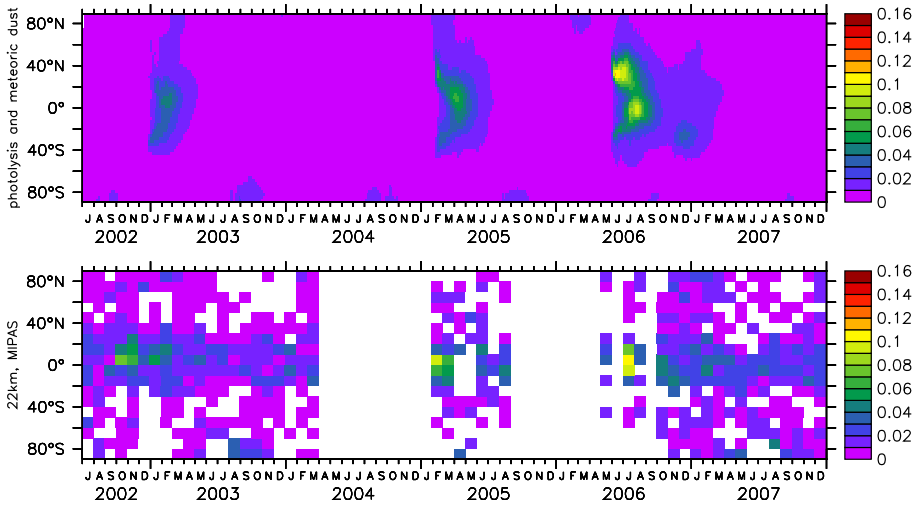

Fig. 14. Simulated and observed SO_2 in the lower stratosphere (22 km).

ACPD
13, 11395–11425, 2013

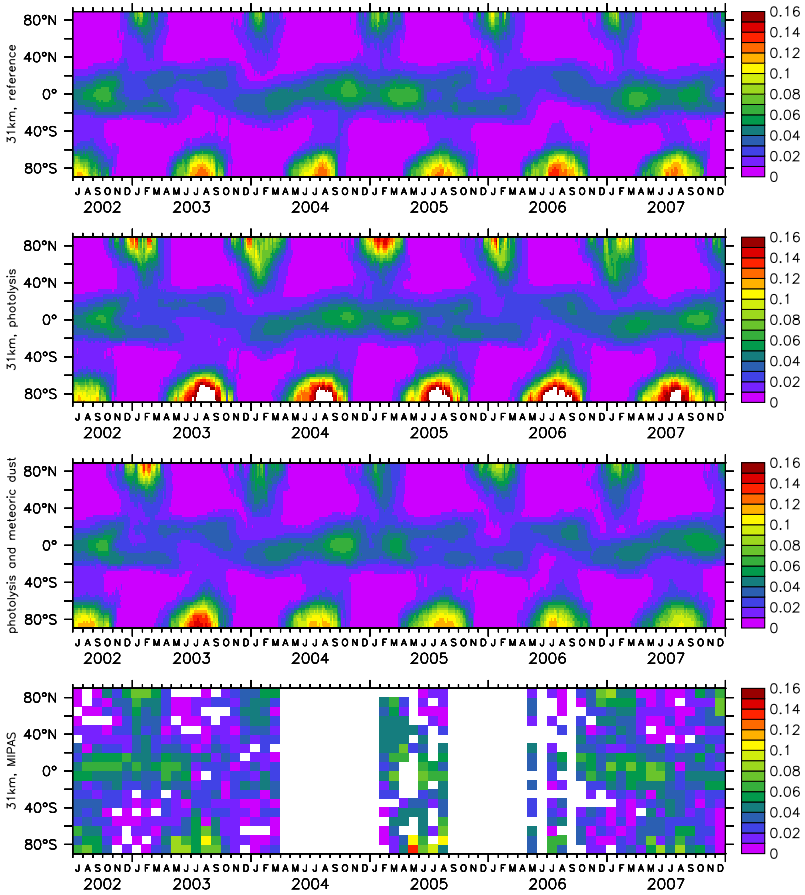

Fig. 15. Simulated and observed (lower panel) SO_2 at 31 km; upper panel as in Brühl et al. (2012), second panel with enhanced H_2SO_4 photolysis and third panel additionally with meteoritic dust sink.

ACPD
13, 11395–11425, 2013

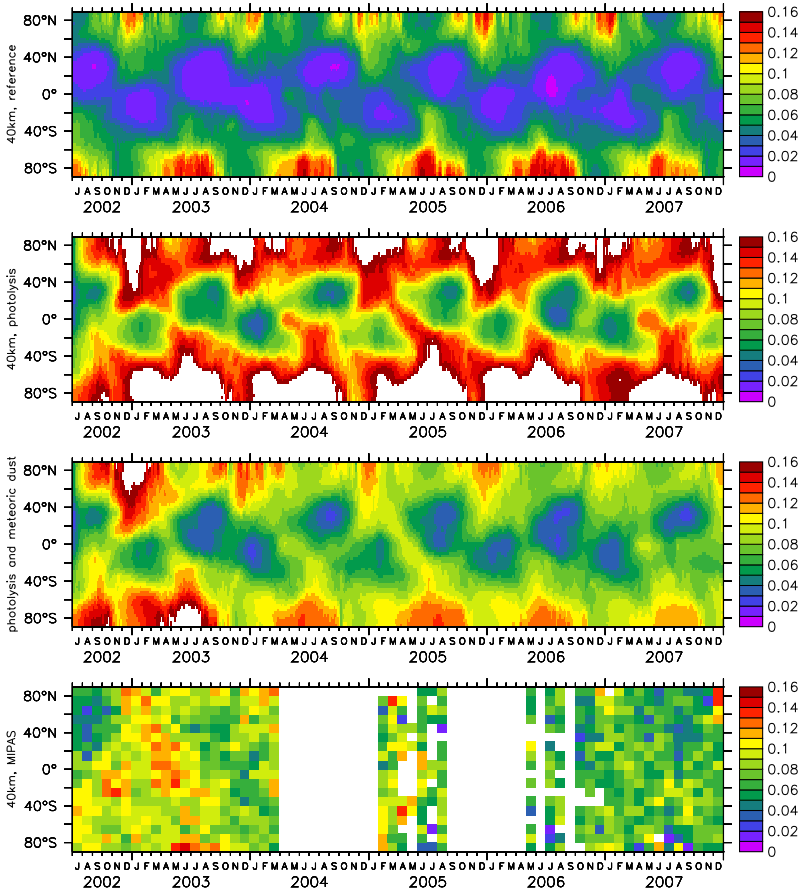

Fig. 16. As Fig. 15 at 40 km.

ACPD
13, 11395–11425, 2013